Use of computed tomography angiography to evaluate the vascular anatomy of the distal portion of the forelimb of horses

Jennifer N. Collins, DVM; Larry D. Galuppo, DVM; Helen L. Thomas, BVMS, DVSc; Erik R. Wisner, DVM; William J. Hornof, DVM, MS

Objective—To provide a detailed description of the vascular anatomy of the distal portion of the forelimbs of horses by use of computed tomography angiography (CTA).

Sample Population—6 forelimbs of 5 horses and 1 forelimb from an equine cadaver; none of the horses had orthopedic or vascular disease.

Procedure—Horses were anesthetized and CTA was conducted on the dependent forelimb. A catheter was inserted in the median artery, and contrast medium was infused at a rate of 3 mL/s. A computed tomography (CT) scanner was used to obtain contiguous slices from the region of the proximal sesamoid bones to the toe. All horses were allowed to recover from anesthesia. To help identify vessel patterns in the distal portion of the forelimb, the median artery and lateral palmar digital vein of a heparinized forelimb obtained from an equine cadaver were infused with red and blue polymethylmethacrylate and the distal portion of that forelimb was then sectioned to correspond to CTA images.

Results—Vessel patterns in CTA images matched vascular anatomic structures of the cadaver forelimb and were consistent with published anatomic structures. Major and minor vessels were consistently visible in CTA images of all horses. There were no complications reported in any horses.

Conclusions and Clinical Relevance—Use of CTA provided a highly detailed depiction of the vasculature of the distal portion of the equine forelimb. This was a safe technique and should be useful in the evaluation of the blood supply to the distal portion of the forelimb. (*Am J Vet Res* 2004;65:1409–1420)

Catastrophic injuries of the bones and soft tissues of the distal portion of the forelimbs are common in horses.[1-9] These injuries are incurred during racing or training or may result from a traumatic incident. Many of these injuries are high-energy events. Concurrent vascular injury is an important complication because ischemic tissue heals more slowly and is at greater risk for developing an infection.[10]

Detrimental effects of vascular compromise in human patients with fractures of the distal portions of the extremities have been reported.[10-17] Infection is among the complications associated with vascular disruption and can result in an increase in morbidity in human patients.[10,12,13] Patients with injuries or conditions in which vascular compromise is suspected are candidates for angiography.[11] Angiography may be indicated in horses for which there is a question regarding vascular injury because severe disruption of the arterial blood supply to the distal portion of the limbs can lead to the need to euthanatize a horse.[18]

The vascular supply of the equine foot has been investigated by use of digital[19,20] and conventional angiography,[21,22] nuclear scintigraphy,[23-25] and Doppler ultrasonography.[26] The information that can be obtained by use of these methods is limited. Conventional and digital radiography provide a 2-dimensional image of a 3-dimensional structure. Radiographs can superimpose vessels on bones, making it difficult to distinguish vascular patterns and integrity of the vessels. Another disadvantage is that a limited number of views can be obtained for each injection of contrast medium in clinical cases. Nuclear scintigraphy provides little information about specific vessels, and Doppler ultrasonography provides no information on complex vascular networks and can be difficult to obtain in patients with traumatic soft tissue injuries.

In humans, **computed tomography angiography (CTA)** has been useful for helping clinicians evaluate the integrity of major arteries of the proximal portion of extremities in patients with traumatic injuries.[11] The authors of that study advocate the use of CTA in patients with a limb that has a diminished but appreciable pulse, a large nonexpanding hematoma, excessive nonpulsatile bleeding, a major neurologic deficit, or ischemia with an appreciable pulse. With the advent of helical **computed tomography (CT)**, many cross-sectional images can be rapidly acquired after a single injection of contrast medium.[27] In 1 study[11] in which investigators evaluated the efficacy of helical CT arteriography as the initial method of diagnosis in human patients suspected of having focal arterial injuries of the proximal portions of the extremities, it was found that CTA had a sensitivity of 95.1% and specificity of 98.7%. Most (137/142 [96.5%]) of these arteriograms were of diagnostic quality, and complications were observed in only 2 of 137 (1.4%) patients.

The use of CT of the distal portions of the limbs

Received December 18, 2003.
Accepted February 20, 2004.
From the Department of Surgical and Radiological Sciences, School of Veterinary Medicine, University of California, Davis, CA 95616.
Dr. Collins' present address is the San Luis Rey Equine Hospital, 4211 Holly Ln Bonsall, CA. 92003.
Supported by the Center for Equine Health, School of Veterinary Medicine, University of California, Davis.
Presented in part at the 30th Annual Convention of the Veterinary Orthopedic Society, Steamboat, Colo, February 2003.
The authors thank John Doval, Jason Peters, and Rich Larson for technical assistance.
Address correspondence to Dr. Collins.

has been described in horses,[28-33] but to our knowledge, there have not been any reports describing selective CTA of the distal portion of the limbs in horses. As CT becomes adopted as a routine procedure by equine clinicians, knowledge of the vascular anatomic structures on CT images may be useful for evaluating vascular integrity in horses with various clinical conditions of the distal portions of the limbs (eg, fractures, lacerations, puncture wounds, injuries to the soft tissues distal to the metacarpophalangeal or metatarsophalangeal [ie, fetlock] joint, osteomyelitis, laminitis, and navicular syndrome).

The objective of the study reported here was to develop an atlas of anatomic structures in the distal portion of the forelimbs of horses by use of a CTA technique. We hypothesized that CTA would be a safe, highly detailed method for evaluating vascular anatomic structures in the distal portion of the forelimbs of horses.

Materials and Methods

Animals—Five horses (2 Standardbreds, 1 Hanoverian, 1 American Paint Horse, and 1 Appaloosa) were used in the study. Horses comprised 4 sexually intact females and 1 castrated male, ranged from 5 to 20 years of age, and weighed between 500 and 694 kg. We conducted CTA twice on the forelimbs of 1 horse; therefore, 6 forelimbs were evaluated in the study. The horses had been donated to the Center for Equine Health at the University of California, Davis, for reasons unrelated to lameness or vascular disease. The study was conducted in accordance with a protocol approved by an animal care and use committee.

CTA—All horses were held off feed for 12 hours before CTA but were allowed unlimited access to water. Horses were sedated by administration of xylazine hydrochloride[a] (0.5 mg/kg, IV), and anesthesia was induced by administration of ketamine hydrochloride[b] (2.2 mg/kg, IV) and guaifenesin[c] (100 mg/kg, IV). After induction, horses were tracheally intubated and anesthesia was maintained with isoflurane and oxygen. The horses were placed in left or right lateral recumbency with the long axis of the limb parallel to the table; all CTA images were obtained on the dependent limb. We obtained data for 6 forelimbs (3 left and 3 right) in 5 horses; both forelimbs were examined in 1 horse. In that horse, there was a 10-week interval between the CTA evaluations of each forelimb. Lateromedial and dorsopalmar localizing views were obtained by use of a helical CT scanner[d] to confirm that the horse was correctly positioned and the entire region to be examined was incorporated in the image. We conducted CT scans before administration of contrast medium; scans extended from just proximal to the proximal sesamoid bones to the distal-most aspect of the distal phalanx and its associated hoof wall. The first forelimb examined was scanned in a distal-to-proximal direction. There was incomplete filling of the palmar digital arteries in the proximal images of that forelimb; therefore, the other 5 forelimbs were scanned in a proximal-to-distal direction. Contiguous transverse images (thickness of 7 mm) were acquired in helical acquisition mode from approximately 1.5 cm proximal to the proximal sesamoid bones to the distal-most aspect of the distal phalanx and its associated hoof wall. Settings for the CT technique were 120 kVp and 150 mA with a scan time of 1 s/slice.

An area (3 cm^2) on the central medial aspect of the antebrachium 3 cm proximal to the medial styloid process in the distal portion of the radius was shaved and aseptically prepared. An 18-gauge, 48-mm arterial catheter[e] was percutaneously inserted into the median artery by use of ultrasonographic[f] guidance. The catheter was secured to the skin with 2-0 polyprolene suture, and a 3-way stopcock[g] was connected to the catheter. An extension set[h] (86 cm in length) was connected to the stopcock and a continuous infusion pump[i] that had a maximum capacity of 100 mL. Iodinated contrast medium[j] (370 mg of iodine/mL) diluted to a 50:50 solution by use of saline (0.9% NaCl) solution was continuously infused at a rate of 3 mL/s but not to exceed 1 mL of total contrast/kg. A volume of 90 to 100 mL of dilute contrast medium was injected during a 30-second period. One horse was injected with nonionic, iodinated contrast medium[k] diluted to a 50:50 solution by use of saline.

We began obtaining CTA images immediately after injection of contrast medium and continued until images of the entire distal portion of the forelimb were obtained. The total time required for scanning of each forelimb was dependent on the distance to be scanned and varied from 32 to 43 seconds.

Patient monitoring—Immediately after completion of CTA, the arterial catheter was removed and a pressure bandage was placed over the site. All horses were monitored during recovery from anesthesia; all horses recovered uneventfully and without assistance. Horses were monitored for 1 week after CTA to detect postinjection complications.

Recording of complications—Procedural complications during CTA were defined as difficulty of infusion, extravasation of contrast medium, acute vasoconstriction, and poor image quality. Image quality was a subjective measurement and was determined by one of the investigators (JNC). Images containing artifacts that obscured the identification of major vessels, bones, or soft tissue structures or in which opacification of vessels was not achieved were considered poor-quality images. Images containing some artifact or minimal extravasation of contrast medium but in which the major vessels, bones, and soft tissues could still be discerned were considered to be of adequate quality. Images in which major and minor vessels were well opacified and bones and soft tissues could be clearly identified were considered to be of excellent quality.

Patient complications were defined as any reaction to the contrast medium or the CTA procedure. Horses were monitored for postinfusion hemorrhage or any vascular-related complication during the 1-week observation period after CTA.

Comparison of CTA images and anatomic structures in a sectioned forelimb from an equine cadaver—The forelimbs of another horse that was euthanatized for reasons unrelated to orthopedic or vascular disease were transected in the middle of the radius. Immediately before being euthanatized, the horse was injected with 300,000 units of sodium heparin.[l] After the forelimbs were harvested, a 14-gauge catheter[e] was inserted in the median artery and the vessels were perfused with heparinized saline solution (3,000 U of heparin/100 mL of saline solution) until the fluid emerging from the veins was clear. The catheter was removed, and a 14-gauge needle was inserted into the median artery, which was infused with red-dyed **polymethylmethacrylate (PMMA).**[m] The lateral palmar digital vein was similarly injected at the level of the proximal phalanx with blue-dyed PMMA. One of the forelimbs was placed in a solution of lye to create a vascular cast. The other forelimb was positioned in a non–weight-bearing position that mimicked the position of the forelimbs in the anesthetized horses during CTA; the appropriately positioned forelimb was frozen at –18°C.

The frozen cadaver forelimb was positioned in the CT gantry in the same position as was used for the forelimbs of the anesthetized horses (ie, the long axis of the limb was parallel to the table). Hand-held cautery devices[n] were used to

make marks at 7-mm increments on the forelimb extending from just proximal to the proximal sesamoid bones to the toe (defined as the distal-most aspect of the distal phalanx). The limb was sectioned with a band saw at 7-mm intervals, and the slices were photographed.[o] Photographed sections were used to help identify the arterial and venous anatomic structure of the CTA images.

All CT images were stored as a data file and transferred to a workstation[p] with 3-dimensional imaging capabilities. Individual images were initially reviewed by use of proprietary software[q] for image analysis with a window width setting of 400 Hounsfield units and a window level of 40 Hounsfield units. Settings for the window width and level were adjusted for each image to optimize resolution of vessels. Evaluation of lamellar vessels of the hoof and vessels within the distal phalanx was accomplished by comparing CTA images with CT images obtained before injection of contrast medium.

Identification of anatomic structures—Eleven regions were selected for analysis on the basis of vascular, soft tissue, and bony structures in the distal portion of the forelimb. These regions consisted of the middle aspect of the proximal sesamoid bones, metacarpophalangeal (ie, fetlock) joint, middle aspect of the proximal phalanx, proximal interphalangeal (ie, pastern) joint, proximal aspect of the middle phalanx, coronary band, distal interphalangeal (ie, coffin) joint, proximal aspect of the distal phalanx, middle aspect of the distal phalanx, distal aspect of the distal phalanx, and the toe (**Figure 1**).

Major vessels were defined as the palmar digital arteries and veins and their main branches. They were identified by comparing CTA images with cadaver specimens (ie, cross-sectional images of the PMMA-injected forelimb and vascular cast of the distal portion of the other forelimb). In addition, published atlases and anatomic textbooks were consulted.[34-42] When a minor vessel (small-diameter vessels or vessels located within tendons, ligaments, or bones) could not be clearly defined on the CTA image, it was identified on the basis of comparison with the CT image obtained before injection of contrast medium. Small-diameter vessels, such as lamellar vessels, coronary vessels, and vessels within the distal phalanx, appeared opaque (white) in the CTA images but did not necessarily appear as distinct vessels. Cortex of the bones and collateral cartilages also appeared white; however, those structures were evident on the CTA images and the CT images obtained before injection of contrast medium. An opacification visible on the CTA image that was not visible on the CT image obtained before injection of contrast medium was suggestive that the structure in question was vascular in origin. Because of the limits of the anatomic cross sections in the distal-most CTA images, vessels in those regions were identified on the basis of comparison with CT images obtained before injection of contrast medium. Major vessels were located and labeled on corresponding CTA images of the 6 forelimbs when they could be clearly identified. Minor vessels (intratendinous and intraligamentous vessels; intertendinous vessels; sesamoidean vessels; dermal vessels; branches of the coronary vessels; branches supplying the ergot, fetlock joint, and digital cushion; and lamellar vessels) were identified and labeled in images in which they were most prominent. Established anatomic terms were used.[40]

Results

Complications—We did not observe complications in any of the horses nor with the CTA procedure. There was 1 poor-quality image in 1 horse. In that horse, the shoe was left on the hoof and metal artifact made the distal-most image unreadable. In the 1 horse in which the forelimb was scanned from distal to proximal, there was incomplete opacification of the palmar digital arteries in the middle aspect of the proximal sesamoid bone and fetlock joint. Because the major structures of the forelimb could still be identified, this was not considered a procedural complication. Although diluted nonionic iodine solution was used in 1 horse, which resulted in a slightly lower iodine concentration, it did not affect image quality.

General results—Results of the study reported here consisted of CTA cross-sectional images through 6 equine forelimbs extending from the proximal sesamoid bones to the toe. There were 32 to 43 cross-sectional images obtained for each forelimb. Number of images varied on the basis of the distance proximal to the proximal sesamoid bones at which we began obtaining CTA images, total length of the region evaluated, and size of the horse.

Vascular anatomic structures were consistent among horses and between left and right forelimbs. Major vessels were consistently identified on the CTA images. There were minor variations evident in filling of the dependent (lateral) and nondependent (medial) ves-

Figure 1—Lateromedial view of the distal portion of the equine forelimb extending from the proximal sesamoid bones to the toe. Selected sites for computed tomography angiographic images were the middle aspect of the proximal sesamoid bones (A), metacarpophalangeal (ie, fetlock) joint (B), middle aspect of the proximal phalanx (C), proximal interphalangeal (ie, pastern) joint (D), proximal aspect of the middle phalanx (E), coronary band (F), distal interphalangeal (ie, coffin) joint (G), proximal aspect of the distal phalanx (H), middle aspect of the distal phalanx (I), distal aspect of the distal phalanx (J), and the toe (defined as the distal-most aspect of the distal phalanx; K).

sels. Slight variations were evident in the location of the branches of the major vessels. Minor vessels were less consistently identified and were associated with more variation in density and location than the major vessels. For all forelimbs, minor vessels were located in the subcutaneous layer and dermis from the middle of the proximal sesamoids bones to the coronary band. These vessels were labeled on images in which they appeared most prominent as dermal vessels and appeared in the dorsal, palmar, lateral, and medial regions.

Proximal sesamoid bones—The major vascular pattern in the region of the middle of the proximal sesamoid bones was consistent among horses (**Figure 2**). The medial and lateral palmar digital arteries were evident in all forelimbs. The medial or lateral palmar digital veins, or both, in 3 of 5 forelimbs scanned from proximal to distal were incompletely opacified, but rentention of contrast medium was sufficient to identify these vessels. In the 1 forelimb scanned from distal to proximal, the medial palmar digital artery had incomplete opacification, the medial palmar digital vein was completely opacified, and the lateral palmar digital artery and vein could not be easily differentiated from each other. In addition, a small intertendinous vessel between the superficial and deep digital flexor tendon was identified in 5 of 6 forelimbs; however, it was observed palmar to the superficial digital flexor tendon in 1 forelimb. Sesamoidean vessels were evident on the abaxial border of the proximal sesamoid bones in all forelimbs.

Fetlock joint—Medial and lateral palmar digital arteries and veins were identified in all forelimbs scanned from proximal to distal (Figure 2). In the 1 forelimb scanned distal to proximal, only the veins were identified. In addition, there was a superficial ramus of the fetlock joint that varied in location and was best seen immediately proximal to the articular surface of the fetlock joint in 2 horses, at the fetlock joint in 1 horse, and distal to the articular surface of the fetlock joint in 3 horses.

The ramus of the ergot was clearly identified in all forelimbs. There were minor variations among forelimbs in the diameter, location, and number of vessels within and between the superficial and deep digital flexor tendons and sesamoidean ligaments on the palmar aspect of the proximal phalanx (Figure 2). Vessels were identified within the common digital extensor tendon in all forelimbs. The palmar ramus of the proximal phalanx was identified in all forelimbs.

Figure 2—Computed tomographic angiographic transverse images of the right forelimb of an anesthetized horse positioned in lateral recumbency (right) and corresponding transverse anatomic sections of the forelimb of an equine cadaver (left; panels A through I) and computed tomographic images before enhancement with contrast agent (left; panels J and K). Images were obtained at regions A through K as illustrated in Figure 1. For images A through F, window width was 1,050 Hounsfield units and window level was 200 Hounsfield units. For images G through K, window width was 750 to 2,000 Hounsfield units and window level was 300 to 900 Hounsfield units. For images J and K, the computed tomography images were obtained at the same window width and window level as the CTA image. Each image is oriented with the lateral aspect to the left and the cranial aspect to the top. 1 = Medial palmar digital artery. 2 = Lateral palmar digital artery. 3 = Medial palmar digital vein. 4 = Lateral palmar digital vein. 5 = Dermal or subcutaneous vessels. 6 = Intertendinous artery. 7 = Sesamoidean vessel. 8 = Ramus of the fetlock joint. 9 = Ramus of the ergot. 10 = Intratendinous vessels. 11 = Intraligamentous vessels. 12 = Palmar ramus of the artery to the proximal phalanx. 13 = Palmar ramus of the vein from the proximal phalanx. 14 = Dorsal ramus of the artery to the proximal phalanx. 15 = Dorsal ramus of middle phalanx. 16 = Palmar ramus of middle phalanx. 17 = Ramus of the digital torus. 18 = Ungular vessels. 19 = Vessels of the digital cushion. 20 = Coronary veins. 21 = Dorsal ramus of the vein from the middle phalanx. 22 = Dorsal ramus of the distal phalanx. 23 = Lamellar vessels. 24 = Circumflex vessels. 25 = Solar foramen. 26 = Branches of the coronary vessels (ie, dermal vessels of the distal phalanx). 27 = Perforating rami. 28 = Terminal arch. CDET = Common digital extensor tendon. DDFT = Deep digital flexor tendon. LPSB = Lateral proximal sesamoid bone. MC III = Third metacarpal bone. MPSB = Medial proximal sesamoid bone. Nav = Navicular bone. ODSL = Oblique distal sesamoidean ligament. P1 = Proximal phalanx. P2 = Middle phalanx. P3 = Distal phalanx. SDFT = Superficial digital flexor tendon. SDSL = Straight distal sesamoidean ligament.

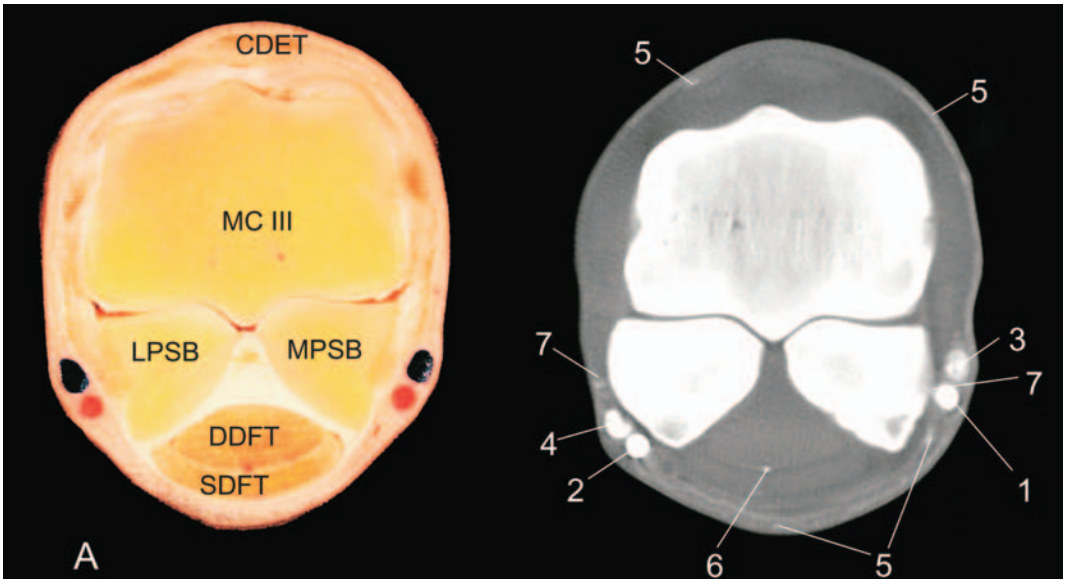

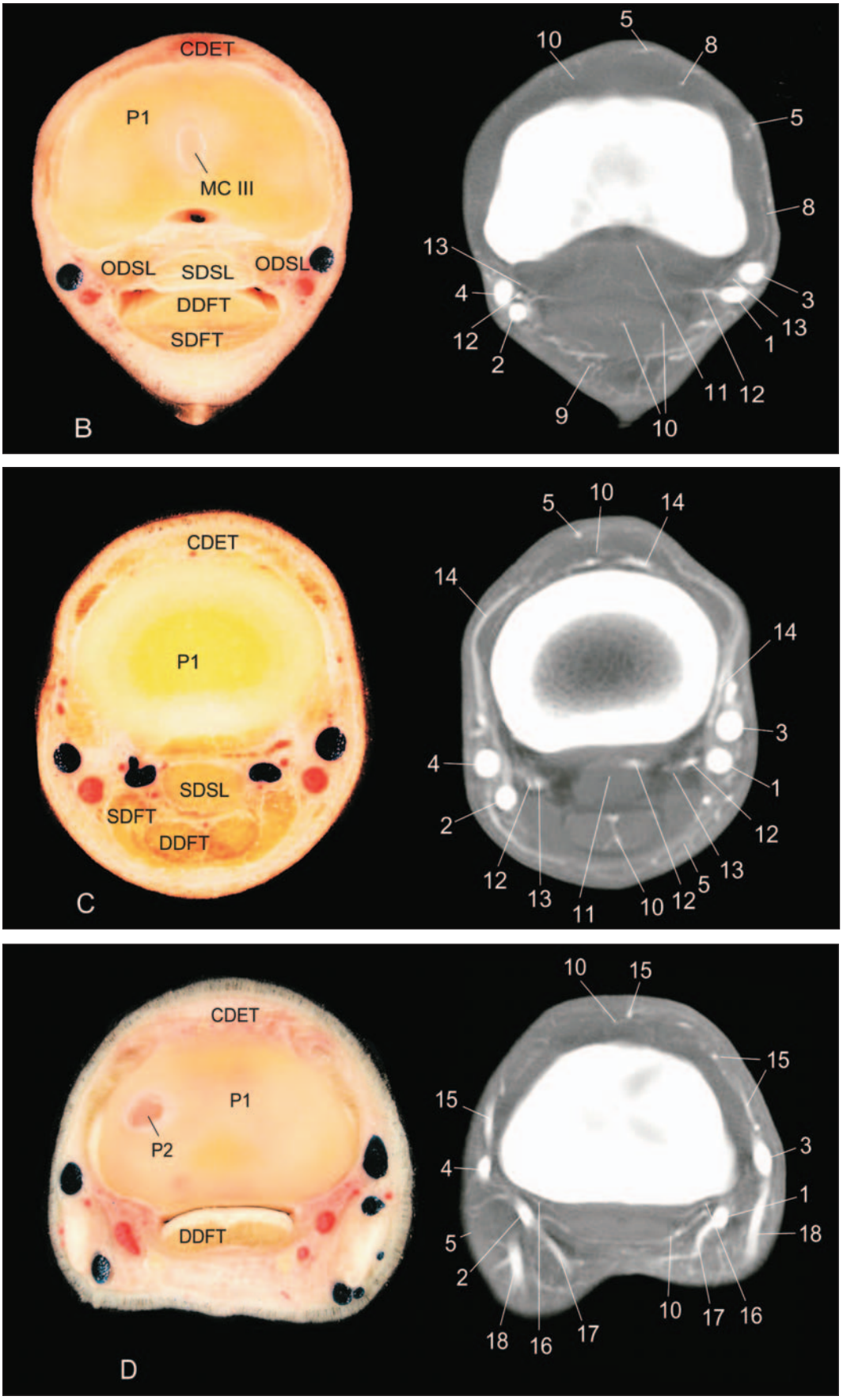

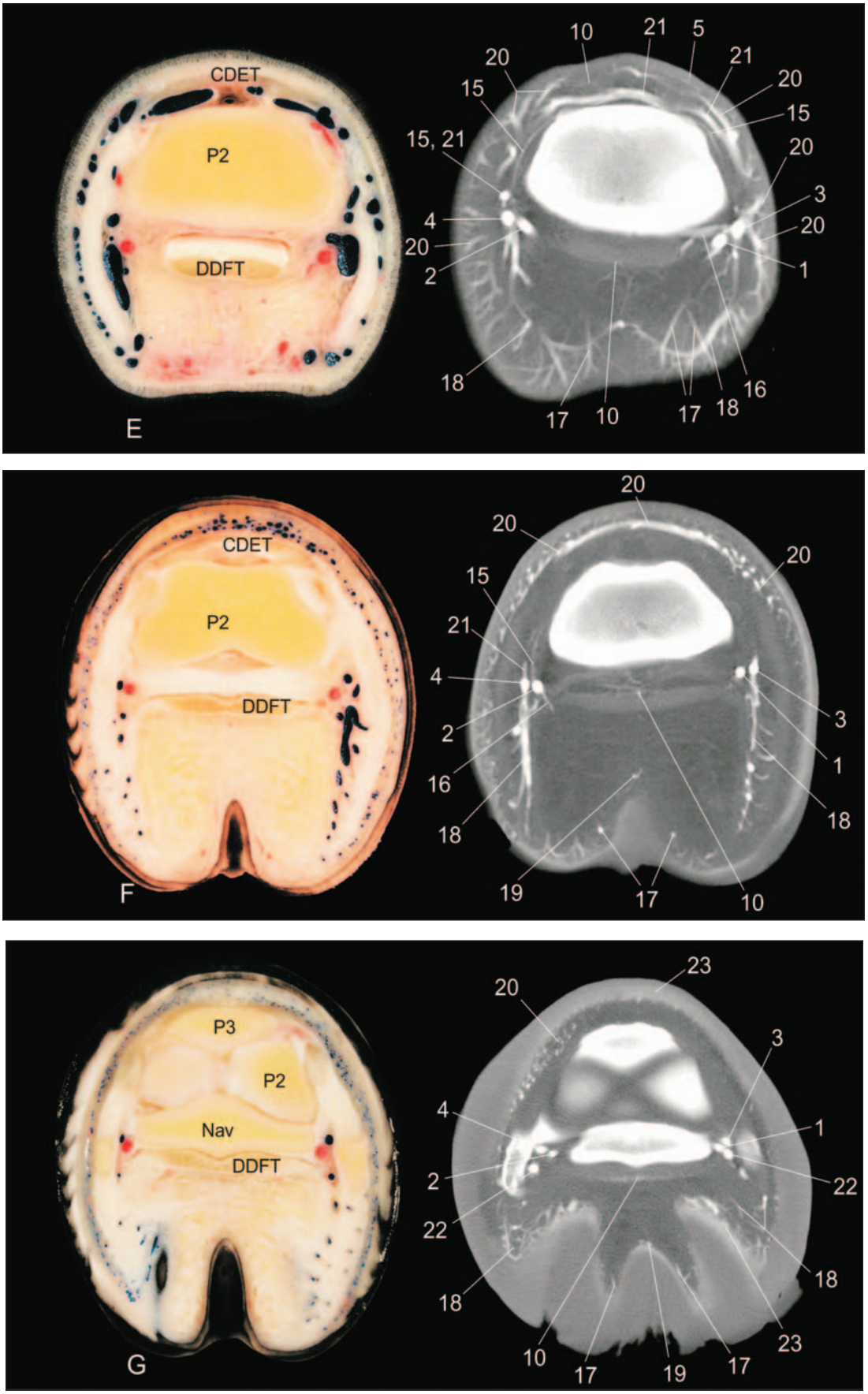

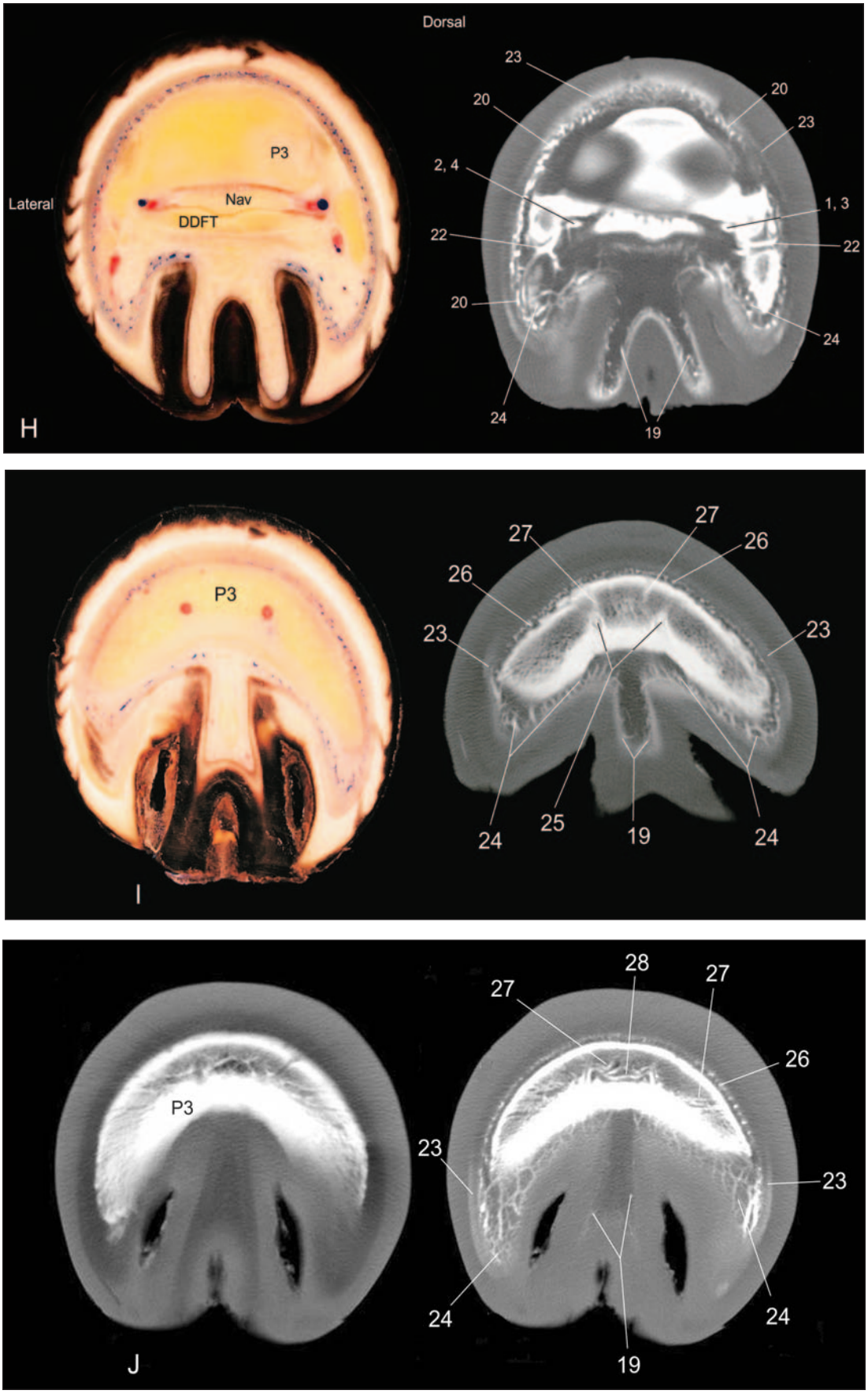

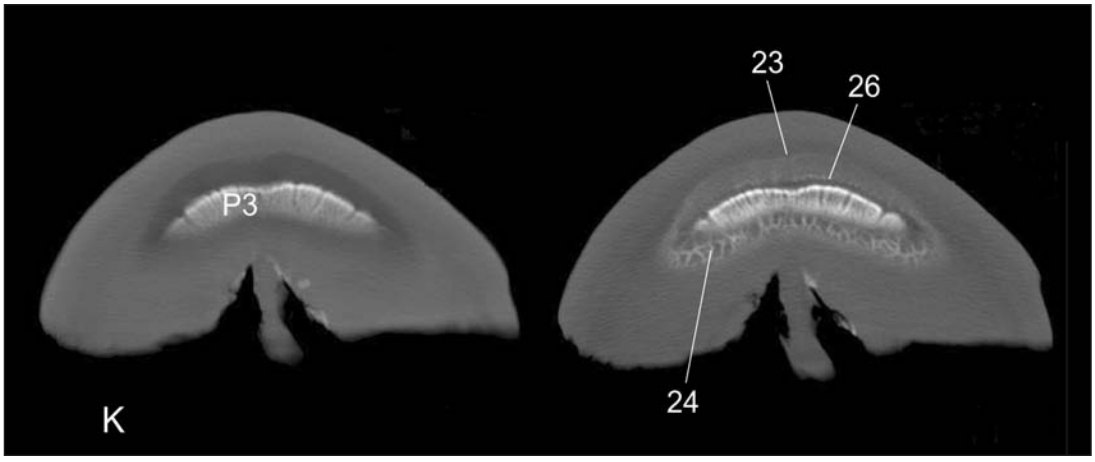

Middle of the proximal phalanx—Medial and lateral palmar digital arteries and veins and minor vessels within the common digital extensor tendon, digital flexor tendons, and ligaments of the distal sesamoids were evident in all forelimbs (Figure 2). In addition, the palmar and dorsal rami of the proximal phalanx could be clearly identified in all forelimbs.

Pastern joint—Medial and lateral palmar digital arteries and veins were evident in all forelimbs (Figure 2). In addition, intratendinous vessels of the common digital extensor tendon and deep digital flexor tendon, palmar and dorsal rami of the middle phalanx, ramus of the digital torus, and ungular vessels were visible in all forelimbs.

Proximal aspect of the middle phalanx—Medial and lateral palmar digital arteries and veins were evident in all forelimbs (Figure 2). In addition, intratendinous vessels of the common digital extensor tendon and deep digital flexor tendon, palmar and dorsal rami of the middle phalanx, ramus of the digital torus, ungular vessels, and coronary vessels were visible in all forelimbs.

Coronary band—Medial and lateral palmar digital arteries and veins were evident in all forelimbs (Figure 2). In addition, the palmar ramus of the middle phalanx, ramus of the digital torus, ungular vessels, vessels of the digital cushion (defined as the terminal branches of the ungular vessels and ramus of the digital torus), and branches of the coronary vessels were visible in all forelimbs. Intratendinous vessels could be discerned in the deep digital flexor tendons of 5 of 6 forelimbs. The dorsal ramus of the middle phalanx was visible in the lateral and medial aspect in 3 forelimbs but only the medial aspect of 2 forelimbs, and it was not clearly identified in 1 forelimb.

Coffin joint—Medial palmar digital artery and vein were evident as separate vessels in 5 of 6 forelimbs; in the other forelimb, these vessels appeared as 1 structure (Figure 2). The lateral palmar digital artery and vein could be identified as separate vessels in all forelimbs. Vessels within the deep digital flexor tendon could be positively identified in all forelimbs. The vascular network of the digital cushion was visible in all forelimbs, and branches of the coronary vessels were visible in the dorsal and lateral aspects of all forelimbs. However, only 4 of 6 forelimbs had branches of coronary vessels visible in the medial (ie, nondependent) aspect of the limb. The dorsal ramus of the distal phalanx was visible in the lateral and medial aspect in 4 forelimbs in which the image was taken at the articular surface. These vessels could not be seen in the 2 images obtained immediately proximal to the joint space. Lamellar vessels were determined by comparison with CT images obtained before injection of contrast medium. Lamellar vessels were evident in all 6 forelimbs. Lamellar vessels could be detected in the dorsal aspect in 5 of 6 forelimbs and in the medial, lateral, and palmar aspects in all forelimbs. Patterns of lamellar vessels varied among forelimbs. In some forelimbs, the lamellar vessels appeared circumferentially around the foot in a halo pattern, whereas opacification of the vessels in other forelimbs was less complete, with only 1 or 2 lamellar regions of the foot becoming opacified in a cluster pattern.

Proximal aspect of the distal phalanx—The proximal aspect of the distal phalanx was characterized in all horses as the last image in which the navicular bone could be viewed. At this point, medial and lateral palmar digital arteries and veins began to enter the distal phalanx and could not always be clearly separated from each other on the CTA images (Figure 2). Vessels of the remaining digital cushion could be identified in all forelimbs. Branches of the coronary vessels could be seen in the dorsal and lateral aspects of the distal phalanx in all forelimbs and in the medial aspect of the distal phalanx in 4 of 6 forelimbs. The dorsal ramus of the distal phalanx was identified entering the lateral and medial palmar process of the distal phalanx in all forelimbs. In all forelimbs, lamellar vessels were identified at the dorsolateral, medial, and palmar aspects of the forelimb. Circumflex vessels were visible in the palmar aspect of the distal phalanx in all forelimbs, and these vessels were more prominent in the lateral (dependent) portion of 3 of 6 forelimbs.

Middle of the distal phalanx—This region was defined by the solar foramen. At this point, terminal vessels of the digital cushion were evident to varying degrees in all forelimbs (Figure 2). Lamellar vessels were

visible in all forelimbs (in clusters at the dorsal, medial, and lateral aspects of 3 forelimbs; circumferentially in 2 forelimbs; and only in the palmarolateral and palmaromedial aspects in 1 forelimb). Circumflex vessels could be clearly discerned in 5 of 6 forelimbs, and they were confirmed by comparison with the CT image obtained before injection of contrast medium in 1 forelimb. The solar foramen was visible biaxially in all forelimbs; however, the vessel in 1 forelimb had to be confirmed by comparison with the CT image obtained before injection of contrast medium. In all forelimbs, dermal vessels, which are distal extensions of the coronary vessels of the distal phalanx, could be seen on the dorsal, lateral, and medial aspects of the distal phalanx, with minor variations in number and diameter. Perforating rami could be identified in 6 forelimbs but were confirmed by comparison with CT images obtained before injection of contrast medium in 4 forelimbs.

Distal aspect of the distal phalanx—Terminal vessels of the digital cushion, lamellar vessels, circumflex vessels, and dermal vessels of the distal phalanx were evident in all forelimbs (Figure 2). The pattern for retention of contrast medium in the dermal and lamellar vessels was variable among and within forelimbs. Perforating rami and the terminal arch were identified in all forelimbs but had to be confirmed by comparison with the CT image obtained before injection of contrast medium in 1 forelimb.

Toe—The toe was defined as the distal-most aspect of the distal phalanx. One image was not readable because of metal artifact from the shoe. Lamellar vessels were evident in all forelimbs (Figure 2). These vessels appeared circumferentially in 3 of 5 forelimbs and had reduced clarity in the dorsal aspect of 2 forelimbs. Circumflex vessels were clearly identified in all forelimbs. Dermal vessels were visible in the dorsal, lateral, and medial aspects of all forelimbs, with 1 forelimb having decreased opacification in the lateral aspect.

Discussion

Computed tomography has become an important diagnostic imaging modality in equine medicine and surgery, and its use in musculoskeletal conditions of horses has been documented.[28-32] In the study reported here, we found that CTA provided a useful technique for development of an atlas of the major and minor vessels of the distal portion of the forelimbs of horses. Vascular patterns observed in this study were identical to those reported elsewhere.[34-42]

Anatomic structures determined by CT of the distal portion of the forelimb have been described,[29] and the use of CT in the diagnosis and evaluation of comminuted fractures of the middle phalanges has been reported.[28] Currently, treatment and prognosis for fractures of the middle phalanges are based largely on configuration of the fracture, degree of comminution, involvement of the distal interphalangeal joint, and the limb (hind limb vs forelimb) involved.[7,28,43] We are not aware of any studies conducted in horses to examine effects of vascular compromise resulting from trauma to the distal portion of the limbs, and it is possible that vessel damage could be an important prognostic indicator in equine patients, similar to the situation in humans. For this reason, imaging techniques that provide quick, accurate observation of the vascular integrity could greatly improve diagnostic and prognostic capabilities when evaluating equine patients with trauma to the distal portions of the limbs. Computed tomography is an accepted method for evaluating damage resulting from trauma of the distal portions of the limbs in horses; however, a working knowledge of the normal anatomic structures evident on CTA images is necessary to effectively evaluate the vessel pattern in these patients.

All images were acquired in helical mode. The helical acquisition mode is faster than the conventional acquisition mode and was necessary for vascular imaging because of the short period that contrast medium remains in the vascular lumen. Total volume injected was dictated by the limits of the infusion pump. We were primarily interested in maintaining intravascular concentrations of contrast medium for the duration of the scan and found that images acquired with helical CTA, a pressure injector with a 100-mL capacity, and an infusion rate of 3 mL of dilute contrast medium/s were adequate for opacification of all major vessels of the distal portion of the forelimbs.

Selection of contrast medium was made on the basis of availability and cost. Ionic iodinated contrast medium is a commonly used contrast medium at our hospital and was less costly than other agents. Because of the exceptional contrast resolution of CT, it was not necessary to use undiluted contrast medium. However, we were conducting multiple scans and chose to dilute the contrast medium to reduce the potential for complications associated with contrast medium.

In the study reported here, we did not detect complications associated with multiple intra-arterial injections of dilute contrast medium through an arterial catheter nor were there any complications associated with the CTA procedure. All horses recovered well from general anesthesia, and there were no postoperative complications associated with the injection site.

Image quality was considered excellent in most cases. There was uptake of contrast medium in the major and minor vessels with no leakage of contrast medium in any forelimb. Dilution of contrast medium (50:50 by use of saline solution) did not appear to affect image quality. Image quality was affected by metal, and the distal-most image was unreadable in the 1 horse in which the shoe was not removed. Thus, shoe removal is recommended to obtain high-quality images. In situations similar to those for our study in which the volume that can be injected is limited, image quality can also be influenced by the direction of scanning. In the 1 forelimb scanned from distal to proximal, there was incomplete opacification of the arteries in images of the proximal portion of the forelimb, and it could be hypothesized that there was incomplete opacification of the branches of these arteries that could potentially have led to an incorrect diagnosis of vascular trauma. This was not considered a procedural complication because the vessels could still be identified; however, we recommend that all limbs be scanned from proximal to distal. In addition, injection of con-

trast medium should begin before the CT scan to ensure perfusion of the palmar digital arteries and veins. Confirmation of complete opacification of the arteries and veins in the proximal-most image will ensure that the contrast medium is still contained in all regions scanned. During review of the images, we frequently adjusted the width and level of the image window to improve visibility of vessels. It was important to ensure the window width and level were the same when comparing CT images obtained before injection of contrast medium with CTA images.

Contiguous transverse images (thickness of 7 mm) obtained in helical mode by use of dilute contrast medium injected at a rate of 3 mL/s were successful for identification of the major vascular pattern of the distal portion of the forelimbs of horses and should provide adequate detail of the vasculature in trauma patients. There is a trade-off between the volume of the anatomic region examined and clarity of the images. Because of summation of tissues in the same plane, image clarity is reduced. Use of narrower collimation would have increased image clarity and allowed for more exact branching patterns to be determined. However, to view the entire distal portion of the forelimb at a narrower collimation, the total time required for imaging would have increased to the point at which it reached the limitations on the CT scanner regarding buildup of heat and cooling needed for the tube. Scans at a thickness of 7 mm can be used for initial evaluation of the blood supply; however, we recommend slices at a thickness of 3 mm or less for more accurate vessel identification (artery vs vein), exact branching locations, and study of specific regions of interest.

One of the main difficulties encountered in the study was the interpretation of the cross-sectional view of the forelimbs. Three-dimensional vascular anatomy was difficult to discern from transverse images. Identification of the vessels was largely determined by reviewing labeled transverse images in a textbook.[34] Although CTA provides excellent vascular imaging, it is difficult to use for identification of veins versus arteries. We referred to published texts,[34,38] constructed PMMA-injected cross-sectional images in the regions of our CTA images, and created a vascular cast to help identify specific vessels. Comparison of PMMA cross sections and CTA images must be made with caution because the cross sections were strict representations of the vascular structures at the exact region where the section was cut, whereas CTA images are representative of the entire 7-mm region. In the CTA images, no information was lost, whereas only surface structures were visible in the cross sections, which allowed investigators to easily miss vessels of small diameter.

Major vessels were identified and labeled as arterial or venous only when this distinction could be clearly discerned by comparing the CTA images with the vascular casts, PMMA cross section, and published materials. Patterns of the major vessels were remarkably consistent in all forelimbs. There were some minor differences among forelimbs. Most differences were detected distal to the coffin joint where vessel diameters were decreased and volume averaging made it difficult to determine intricate branching patterns. The dorsal ramus of the distal phalanx was not clear in 2 forelimbs, but this was probably attributable to the fact that the CTA image was taken proximal to the joint space. In all forelimbs imaged directly through the coffin joint, the ramus of the distal phalanx was visible in the medial and lateral aspects. For images obtained at the coronary band, the dorsal ramus of the middle phalanx was not consistently detected. In this region, the vessel is a small-diameter vessel. This was most likely attributable to typical variation in vessel anatomy and spacing of the CTA images and did not reflect a true perfusion deficit. In the region of the coffin joint, volume averaging precluded the distinction of the palmar digital artery from the vein on the nondependent side in 1 forelimb. At the proximal aspect of the distal phalanx, close proximity and small diameter of palmar digital arteries and veins made it difficult to distinguish the arteries and veins as separate vessels at the point where they begin to enter the distal phalanx. In the region of the middle aspect of the distal phalanx, there was some variation in the location of the solar foramen. Arteries[36,38] and veins[37] reportedly are within the solar foramen. In the study reported here, tissue summation did not allow for the distinction of arteries from veins within the solar foramen. The specimen injected with PMMA was an arterial structure, suggesting that the artery was most likely the vessel within the canal identified in the CTA image. The distal aspect of the distal phalanx and toe were primarily evaluated by comparison with CT images obtained before injection of contrast medium because the vessel patterns within the distal phalanx were difficult to determine. For this region, increasing the magnification and varying the window width and level allowed for confirmation of the terminal arch, perforating rami, and circumflex vessels in all forelimbs.

In addition to identification of major vessels, our technique was successful for use in determining small-diameter vessels, lamellar vessels, intratendinous and intraligamentous vessels, and regional vascular networks. There was greater variability in retention of contrast medium in these minor vessels, especially those distal to the coffin joint. Some of the variation observed was most likely related to conditions not specifically controlled for by the study, such as cardiac output and depth of anesthesia. In addition, we did not control the amount of vasodilatory agents (eg, xylazine) used for induction of general anesthesia.

Distal to the coronary band in all forelimbs, the minor vessels on the dependent (lateral) portion of the forelimbs had a tendency to have greater opacification than was evident on the nondependent (medial) portion. Because the lateral aspect of the forelimb was always dependent, it was not possible to conclude whether the differences observed were related to the effects of gravity or were actual anatomic differences between the lateral and medial aspects of the limbs. However, on the basis of results from other studies in which investigators evaluated blood flow to the equine digit during lateral recumbency[36] and in standing cadaveric limbs,[19] no mention was made of differences between the medial and lateral side of the forelimb.

Thus, these differences are likely associated with the gravitational influence on iodinated contrast media.

A second observation associated with the minor vessels was the wide variation of perfusion patterns among forelimbs for the lamella and branches of the coronary vessels (dermal vessels) of the distal phalanx. Vascular supply to the equine digit is complex, and the dorsal and palmar aspects of the foot have differing and highly intricate blood supplies and drainage patterns.[36,38] For example, vessels supplying the dorsal lamella must travel through the distal phalanx, and perfusion of these lamella is in a distal-to-proximal direction, whereas the palmar lamella receive their blood supply directly from the coronary vessels and are perfused in a proximal-to-distal direction. In addition, there are several small valves within the coronary and ungular vessels that allow blood to leave the foot via many routes.[38] Because microcirculation patterns of the foot are highly variable, the differences in vessel opacification we observed were most likely a reflection of typical variations and did not indicate perfusion deficiencies.

In the study reported here, we found CTA to be a safe, relatively simple, highly effective method for obtaining high-quality images that will allow clinicians to evaluate the vascular supply to the distal portion of the equine forelimb. As CT becomes more routine in equine practice, knowledge of the anatomic structures of the distal portion of the forelimbs visible on CTA images is likely to be useful in the evaluation of vascular patterns for various clinical conditions.

[a]Tranqui-vet, Vedco Inc, St Joseph, Mo.
[b]Ketaved, Phoenix Scientific, St Joseph, Mo.
[c]Guaifenesin, Phoenix Scientific, St Joseph, Mo.
[d]GE 9800 quick helical CT scanner, GE Medical Systems, Milwaukee, Wis.
[e]Angiocath, Becton-Dickinson, Sandy, Utah.
[f]10.0 MHz Ausonics microconvex probe, Universal Medical, Bedford Hills, NY.
[g]Ez-Flo, Sherwood Medical, St Louis, Mo.
[h]Extension set, Baxter, Deerfield, Ill.
[i]Cordis flow rate injector, model 187a, KD Scientific Inc, Boston, Mass.
[j]RenoCal, 370 mg/mL, ER Sqiubb & Sons Inc, New Brunswick, NJ.
[k]Isovue-300, 300 mg/mL, Squibb Diagnostics, Princeton, NJ.
[l]Heparin, Elkin-Sinn Inc, Cherry Hill, NJ.
[m]Coetray plastic, GC America, Chicago, Ill.
[n]Acu-Dispo cautery, Acuderm Inc, Fort Lauderdale, Fla.
[o]Nikkon DIX, 60-mm macro lens, Nikkon, Tokyo, Japan.
[p]GE Advantage 3.1 software, Sun Microsystems, Silicon Valley, Calif.
[q]Efilm, Merge Technologies Inc, Milwaukee, Wis.

References

1. Estberg L, Stover SM, Gardner IA, et al. Fatal musculoskeletal injuries incurred during racing and training in Thoroughbreds. *J Am Vet Med Assoc* 1996;208:92–96.

2. Johnson BJ, Stover SM, Daft BM, et al. Causes of death in racehorses over a 2 year period. *Equine Vet J* 1994;26:327–330.

3. Hernandez J, Hawkins DL, Scollay MC. Race-start characteristics and risk of catastrophic musculoskeletal injury in Thoroughbred racehorses. *J Am Vet Med Assoc* 2001;218:83–86.

4. Hill AE, Stover SM, Gardener IA, et al. Risk factors for and outcomes of noncatastrophic suspensory apparatus injury in Thoroughbred racehorses. *J Am Vet Med Assoc* 2001;218:1136–1144.

5. Peloso JG, Mundy GD, Cohen ND. Prevalence of, and factors associated with, musculoskeletal racing injuries of Thoroughbreds. *J Am Vet Med Assoc* 1994;204:620–626.

6. Pool RR, Meagher DM. Pathologic findings and pathogenesis of racetrack injuries. *Vet Clin North Am Equine Pract* 1990;6:1–30.

7. Watkins JP. Fractures of the middle phalanx. In: Nixon AJ, ed. *Equine fracture repair*. Philadelphia: WB Saunders Co, 1996;129–145.

8. Wilson JH, Robinson RA, Jensen RC, et al. Equine soft tissue injuries associated with racing descriptive statistics from American racetracks. In: Rantanen NW, Hauser ML, eds. *Dubai international equine symposium. The equine athlete: tendon, ligament and soft tissue injuries*. Bonsall, Calif: Matthew R Rantanen Design, 1996;1–21.

9. Zekas LJ, Bramlage LR, Emberson RM, et al. Characterisation of the type and location of fractures of the third metacarpal/metatarsal condyles in 135 horses in central Kentucky (1986– 1994). *Equine Vet J* 1999;31:304–308.

10. Alexander JJ, Piotrowski JJ, Graham D, et al. Outcome of complex vascular and orthopedic injuries of the lower extremity. *Am J Surg* 1991;162:111–116.

11. Soto JA, Munera F, Morales C, et al. Focal arterial injuries of the proximal extremities: helical CT arteriography as the initial method of diagnosis. *Radiology* 2001;218:188–194.

12. Bandyk DF. Vascular injury associated with extremity trauma. *Clin Orthop Relat Res* 1995;318:117–124.

13. Gustilo RB, Mendoza RM, Williams DN. Problems in the management of type III (severe) open fractures: a new classification of type III open fractures. *J Trauma* 1984;24:742–746.

14. Winkelaar GB, Taylor DC. Vascular trauma associated with fractures and dislocations. *Semin Vasc Surg* 1998;11:261–273.

15. Sriussadaporn S. Arterial injuries of the lower extremity from blunt trauma. *J Med Assoc Thai* 1997;80:121–129.

16. al-Salman MM, al-Khawashki H, Sindigki A, et al. Vascular injuries associated with limb fractures. *Injury* 1997;28:103–107.

17. Johansen K, Daines M, Howey T, et al. Objective criteria accurately predict amputation following lower extremity trauma. *J Trauma* 1990;30:568–573.

18. Scott EA, Sandler GA, Shires MH. Angiography as a diagnostic technique in the equine. *J Equine Med Surg* 1978;37:869–873.

19. Rosenstein DS, Bowker RM, Bartlett PC. Digital angiography of the feet of horses. *Am J Vet Res* 2000;61:255–259.

20. Redden RF. A technique for performing digital venography in the standing horse. *Equine Vet Educ* 2001;13:128–134.

21. Scott EA, Thrall DE, Sandler GA. Angiography of equine metacarpus and phalanges: alterations with medial palmar artery and medial palmar digital artery ligation. *Am J Vet Res* 1976; 37:869–873.

22. Ackerman N, Garner HE, Coffman JR, et al. Angiographic appearance of the normal equine foot and alterations in chronic laminitis. *J Am Vet Med Assoc* 1975;166:58–62.

23. Dyson S, Lakhani K, Wood J. Factors influencing blood flow in the equine digit and their effect on uptake of 99m technetium methylene diphosphonate into bone. *Equine Vet J* 2001;33:591–598.

24. Trout DR, Hornof WJ, Linford RL, et al. Scintigraphic evaluation of digital circulation during the developmental and acute phases of equine laminitis. *Equine Vet J* 1990;22:416–421.

25. Galey FD, Twardock AR, Goetz TE, et al. Gamma scintigraphic analysis of the distribution of perfusion of blood in the equine foot during black walnut (*Juglans nigra*)-induced laminitis. *Am J Vet Res* 1990;51:688–695.

26. Adair HS, Goble DO, Shires GM, et al. Evaluation of laser Doppler flowmetry for measuring coronary band and laminar microcirculatory blood flow in clinically normal horses. *Am J Vet Res* 1994;55:445–449.

27. Seeram E. Computed tomography angiography: technical considerations. In: Seeram E, ed. *Computed tomography: principles, clinical applications, and quality control*. Philadelphia: WB Saunders Co, 1994;173–197.

28. Rose PL, Seeherman H, O'Callaghan M. Computed tomographic evaluation of comminuted middle phalangeal fractures in the horse. *Vet Radiol Ultrasound* 1997;38:424–429.

29. Peterson RP, Bowman KF. Computed tomographic anatomy of the distal extremity of the horse. *Vet Radiol* 1988;29:147–156.

30. Barbee DD, Allen JR, Gavin PR. Computed tomography in horses. *Vet Radiol* 1987;28:144–151.

31. Tucker RL, Sande RD. Computed tomography and magnetic resonance imaging in equine musculoskeletal conditions. *Vet Clin North Am Large Anim Pract* 2001;17:145–157.

32. Whitton RC, Buckley C, Donovan T, et al. The diagnosis of lameness associated with distal limb pathology in the horse: a com-

parison of radiography, computed tomography and magnetic resonance imaging. *Vet J* 1998;155:223–229.

33. Widmer WR, Buckwalter KA, Fessler JF, et al. Use of radiography, computed tomography and magnetic resonance imaging for evaluation of navicular syndrome in the horse. *Vet Radiol Ultrasound* 2000;41:108–116.

34. Denoix JM. *The equine distal limb: an atlas of clinical anatomy and comparative imaging*. Ames, Iowa: Iowa State University Press, 2000.

35. Schaller O. Angiologia. In: Schaller O, ed. *Illustrated veterinary anatomical nomenclature*. Stuttgart, Germany: Ferdinand Enke Verlag, 1992;334–371.

36. Colles CM, Garner HE, Coffman JR. The blood supply of the horse's foot, in *Proceedings*. 25th Annu Meet Am Assoc Equine Pract 1980;385–389.

37. Mishra PC, Leach DH. Extrinsic and intrinsic veins of the equine hoof wall. *J Anat* 1983;136:543–560.

38. Pollitt CC. Structure and function. In: Pollitt CC, ed. *Color atlas of the horse's foot*. London: Mosby-Wolfe, 1995;9–27.

39. Ghoshal NG, Getty R. The arterial blood supply to the appendages of the horse. *Iowa State J Vet Sci* 1968;43:153–181.

40. World Association of Veterinary Anatomists. Angiologia in equus. In: *Nomina anatomica veterinaria*. 4th ed. Ithaca, NY: International Committee on Veterinary Gross Anatomic Nomenclature, 1994;300–301.

41. Trumble TN, Arnoczky SP, Stick JA, et al. Clinical relevance of the microvasculature of the equine proximal sesamoid bone. *Am J Vet Res* 1995;56:720–724.

42. Kraus BL, Kirker-Head CA, Kraus KH, et al. Vascular supply of the tendon of the deep digital flexor muscle within the digital sheath. *Vet Surg* 1995;24:102–111.

43. Stashak T. Fractures of the middle phalanx. In: Stashak T, ed. *Adams lameness in horses*. 5th ed. Philadelphia: Lippincott Williams & Wilkins, 2002;744–754.